Constraining the interior of neutron stars from their tidal deformations and oscillations

Aurélien Sourie

Institut d'Astronomie et d'Astrophysique
Université Libre de Bruxelles

Villa Tambosi (Trento) - October 16, 2019

1. Neutron stars and gravitational waves

2. The first direct detection of gravitational waves from a binary neutron-star merger & tidal deformabilities
in collaboration with N. Chamel and L. Perot (ULB)

3. Modelling neutron-star oscillations with spectral methods
in collaboration with J. Novak, M. Oertel and E. Declerck (LUTH)

4. Conclusions

Equations of state

Several equations of state (EoSs) have been proposed to account for the current uncertainties in the composition of neutron stars (NSs) and in the interactions between their constituants.

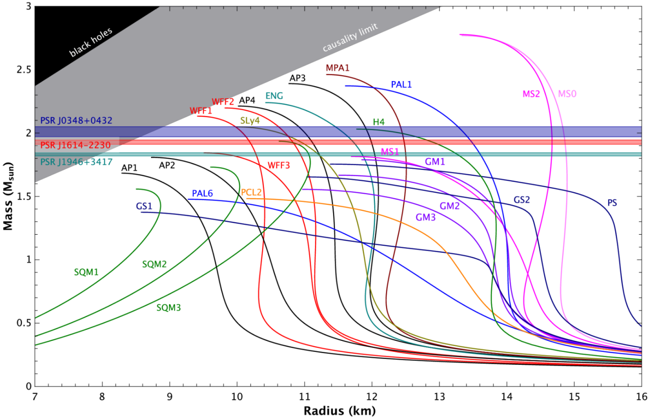

https://www3.mpifr-bonn.mpg.de/staff/pfreire/NS_masses.html

Gravitational waves from neutron stars

Neutron stars are excellent emitters of gravitational waves.

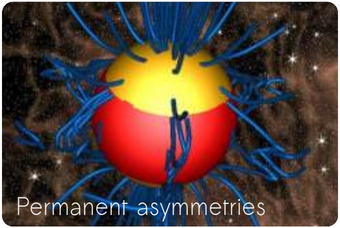

1. Neutron stars and gravitational waves

2. The first direct detection of gravitational waves from a binary neutron-star merger & tidal deformabilities
in collaboration with N. Chamel and L. Perot (ULB)

3. Modelling neutron-star oscillations with spectral methods
in collaboration with J. Novak, M. Oertel and E. Declerck (LUTH)

4. Conclusions

GW170817

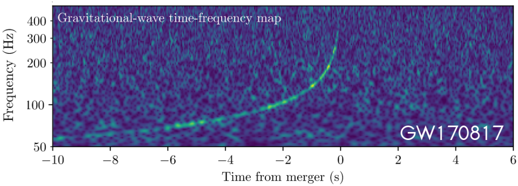
Gravitational-wave time-frequency map
GW170817
Frequency (Hz)
400
300
200
100
50
−10
−8
−6
−4
−2
0
2
4
6
Time from merger (s)

GW170817

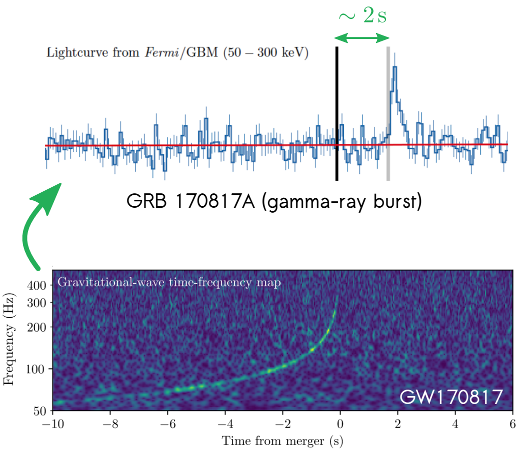
~ 2 s
Lightcurve from Fermi/GBM (50 – 300 keV)
GRB 170817A (gamma-ray burst)
Gravitational-wave time-frequency map
GW170817
Frequency (Hz)
400
300
200
100
50
−10
−8
−6
−4
−2
0
2
4
6
Time from merger (s)

GW170817

a few hours/days later

$\sim 2\,\mathrm{s}$

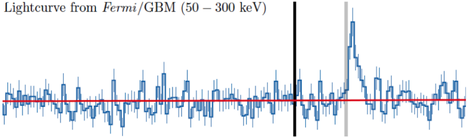

GRB 170817A (gamma-ray burst)

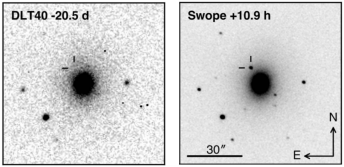

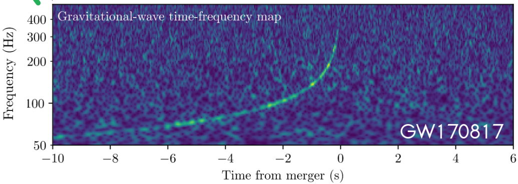

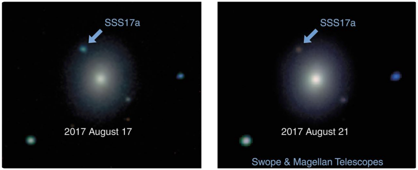

kilonova (AT 2017gfo)

Tidal deformabilities

During the last orbits preceding the merger, the two neutron stars are strongly deformed by tidal effects.

Tidal deformabilities

Tidal effects are encoded by the coefficient $\tilde{\Lambda} = \tilde{\Lambda}(M_1, M_2, \Lambda_1, \Lambda_2)$. Each individual tidal deformability Λ_i depends on M_i and the EoS.

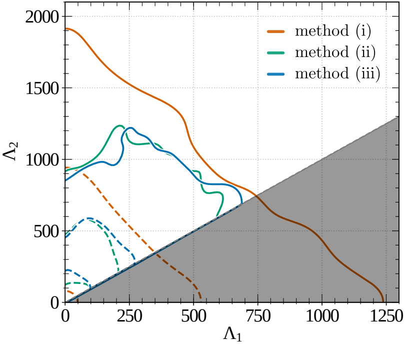

LVC, *PRL* **121**, 161101 (2018)

Analysis of the GW170817 signal by the LIGO/Virgo collaboration:

(i) M_1, M_2, Λ_1 & Λ_2 are treated independently,

(ii) Λ_1, Λ_2 & M_2/M_1 are related by a universal relation,

(iii) a large set of parametrised EoSs is used, assuming a common EoS for the two NSs.

Unified EoSs

The BSk EoSs provide a unified and thermodynamically consistent treatment of all regions of the NS and are calculated using functionals that are precision fitted to experimental and theoretical nuclear data.

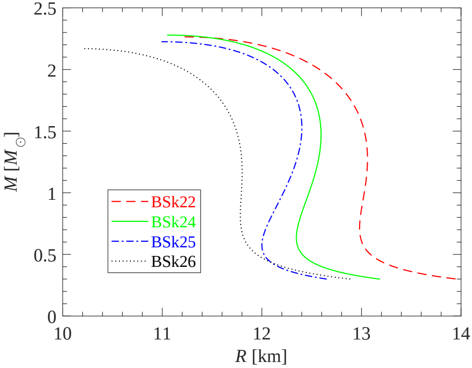

Pearson *et al.*, *MNRAS* **481** (2018)

- BSk22, BSk24 & BSk25 mainly differ in their predictions for the symmetry energy [$J = 32$, 30 & 29 MeV] but are fitted to the same NeuM EoS [LS2].

- BSk26 is fitted to the same symmetry-energy coefficient at saturation as BSk24 but to a softer NeuM EoS [APR].

Constraints on the tidal deformabilities

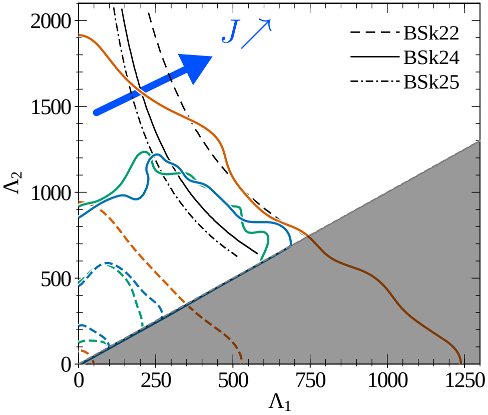

Perot *et al.*, *PRC* **100** (2019)

★ BSk22, with a symmetry energy coefficient $J = 32$ MeV and a slope $L = 68.5$ MeV, appears to be *disfavored*.

Constraints on the tidal deformabilities

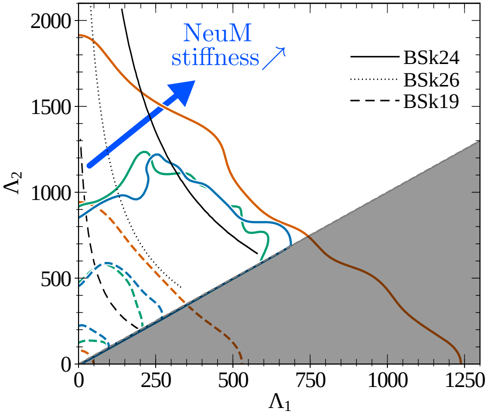

Perot *et al.*, *PRC* **100** (2019)

★ BSk22, with a symmetry energy coefficient $J = 32$ MeV and a slope $L = 68.5$ MeV, appears to be *disfavored*.

★ Predictions from the older BSk19 EoS, fitted to a *very soft* NeuM EoS, are consistent with the GW170817 constraints, *even though this EoS does not support* $2M_\odot$ *NSs!*

The GW data alone tend to favor a rather soft EoS at densities relevant for medium-mass NSs.

Constraints on the structure of nonrotating NSs

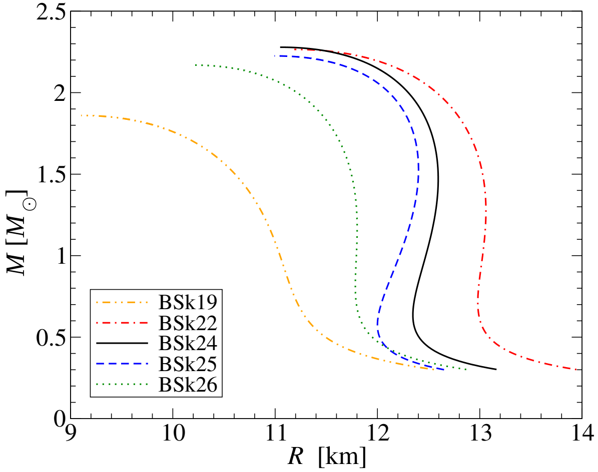

Perot *et al.*, *PRC* **100** (2019)

Constraints on the structure of nonrotating NSs

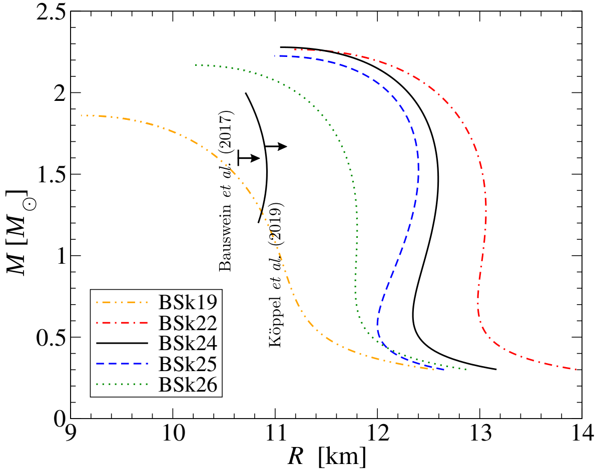

Perot *et al.*, *PRC* **100** (2019)

♠ No prompt collapse to a black hole [EM] ⇝ *R*,

Constraints on the structure of nonrotating NSs

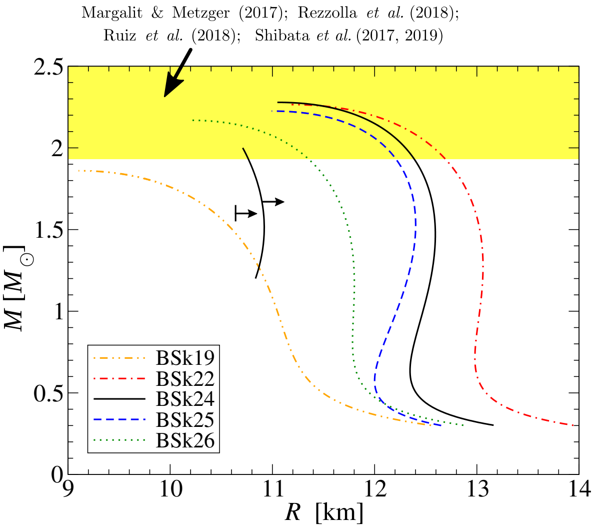

Perot *et al.*, *PRC* **100** (2019)

♠ No prompt collapse to a black hole [EM] $\rightsquigarrow$ R,

♠ Formation of a short-lived hyper- or supramassive NS [EM] $\rightsquigarrow$ M_{max},

but lack of consensus about the interpretation of the EM data...

Constraints on the structure of nonrotating NSs

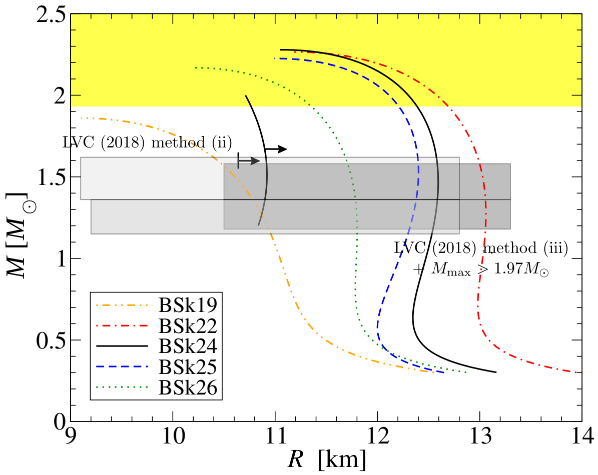

Perot *et al.*, *PRC* **100** (2019)

♠ No prompt collapse to a black hole [EM] ⇝ R,

♠ Formation of a short-lived hyper- or supramassive NS [EM] ⇝ $M_{\rm max}$,

but lack of consensus about the interpretation of the EM data...

♠ Constraints on tidal deformabilities [GW] ⇝ R.

Why modelling neutron-star oscillations?

Several oscillation modes are likely to be excited during violent events such as core-collapse supernovae or neutron-star mergers.

$\rightsquigarrow$ **asteroseismology**

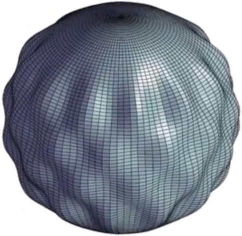

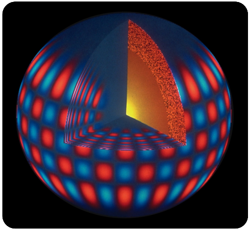

This project aims at computing accurate gravitational-wave spectra associated with the pulsations of an isolated rotating neutron star, for a whole set of realistic EoSs.

Different strategies

- Mode-frequencies are usually computed using *perturbation theory*.

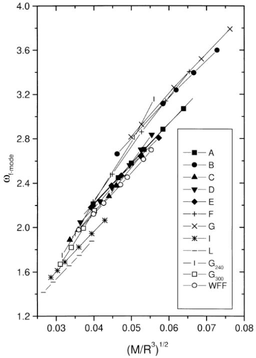

Andersson & Kokkotas, *MNRAS* **299** (1998)

Different strategies

- Mode-frequencies are usually computed using *perturbation theory*.

- An alternative approach is to solve the *time-evolution of the non-linear equations* governing the dynamics of matter and spacetime.

⇝ Dimmelmeier *et al.* (2006) used CoCoNuT to compute non-linear axisymmetric pulsations of rotating relativistic NSs for polytropic EoSs.

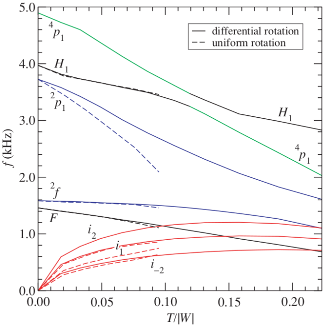

Dimmelmeier *et al.*, *MNRAS* **368** (2006)

Different strategies

- Mode-frequencies are usually computed using *perturbation theory*.

- An alternative approach is to solve the *time-evolution of the non-linear equations* governing the dynamics of matter and spacetime.

⇝ Dimmelmeier *et al.* (2006) used CoCoNuT to compute non-linear axisymmetric pulsations of rotating relativistic NSs for polytropic EoSs.

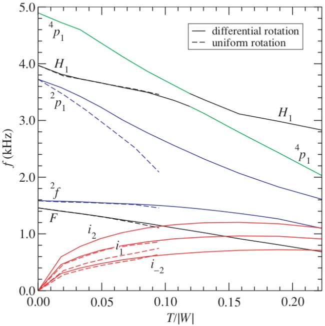

Dimmelmeier *et al.*, *MNRAS* **368** (2006)

Contrary to previous studies, we plan to use spectral methods to solve *both* the hydrodynamic & metric equations in order to *reduce* computing times considerably.

Numerical procedure

So far, the code is based on Newtonian gravity in spherical symmetry and makes use of polytropic EoSs ($\gamma = 2$).

- Continuity eq.:

$$\frac{\partial \rho}{\partial t} = -\frac{1}{r^2}\frac{\partial}{\partial r}\left(r^2 v \rho\right)$$

- Euler eq.:

$$\frac{\partial v}{\partial t} = -v\frac{\partial v}{\partial r} - \frac{1}{\rho}\frac{\partial p}{\partial r} - \frac{\partial \Phi}{\partial r}$$

- Poisson eq.:

$$\Delta\Phi = 4\pi G\rho$$

- EoS:

$$p = \kappa\rho^{\gamma}$$

Numerical procedure

So far, the code is based on Newtonian gravity in spherical symmetry and makes use of polytropic EoSs ($\gamma = 2$).

- Continuity eq.:

$$\frac{\partial \rho}{\partial t} = -\frac{1}{r^2}\frac{\partial}{\partial r}\left(r^2 v \rho\right)$$

- Euler eq.:

$$\frac{\partial v}{\partial t} = -v\frac{\partial v}{\partial r} - \frac{1}{\rho}\frac{\partial p}{\partial r} - \frac{\partial \Phi}{\partial r}$$

- Poisson eq.:

$$\Delta \Phi = 4\pi G \rho$$

- EoS:

$$p = \kappa \rho^{\gamma}$$

- Boundary condition at $R_\star = R(t)$:

$$\rho(R_\star, t) = const$$

OR $$\frac{1}{r^2}\frac{\partial}{\partial r}\left(r^2 v\right)(R_\star, t) = 0$$

Numerical procedure

So far, the code is based on Newtonian gravity in spherical symmetry and makes use of polytropic EoSs ($\gamma = 2$).

- Continuity eq.:

$$\frac{\partial \rho}{\partial t} = -\frac{1}{r^2}\frac{\partial}{\partial r}\left(r^2 v \rho\right)$$

- Euler eq.:

$$\frac{\partial v}{\partial t} = -v\frac{\partial v}{\partial r} - \frac{1}{\rho}\frac{\partial p}{\partial r} - \frac{\partial \Phi}{\partial r}$$

- Poisson eq.:

$$\Delta \Phi = 4\pi G \rho$$

- EoS:

$$p = \kappa \rho^{\gamma}$$

- Boundary condition at $R_\star = R(t)$:

$$\rho(R_\star, t) = const$$

OR

$$\frac{1}{r^2}\frac{\partial}{\partial r}\left(r^2 v\right)(R_\star, t) = 0$$

★ pseudo-spectral methods with Chebyshev polynomials (LORENE),

★ time-integration with a 3rd-order Adams-Bashforth method,

★ moving grid adapted to the stellar surface.

Exciting oscillation modes

1. Start from an equilibrium configuration,

2. Induce a perturbation in the fluid properties so as to excite some particular oscillation modes,

3. Follow the time evolution of a fluid variable (the central density or the radius, here).

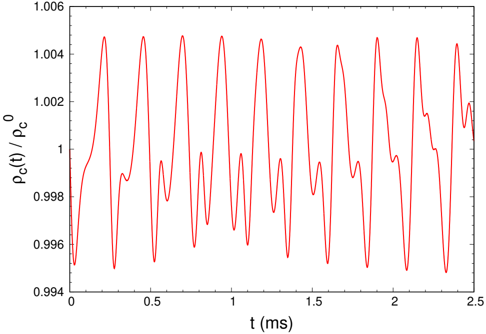

♠ Stellar configuration: $\rho_c^0 = 1.9891 \times 10^{18}$ kg m^{-3}, $\kappa = 4.25 \times 10^{-3}$ m^5 kg^{-1} s^{-2}

♠ Initial perturbation: $v(r, 0) = v_0 \sin(\pi r / R_0)$ with $v_0 = 300$ km s^{-1}

♠ Numerical parameters: $n_r = 25$, $\delta t = 5 \times 10^{-5} \times t_h$ (where $t_h \sim 0.08$ ms)

Exciting oscillation modes

1. Start from an equilibrium configuration,

2. Induce a perturbation in the fluid properties so as to excite some particular oscillation modes,

3. Follow the time evolution of a fluid variable (the central density or the radius, here).

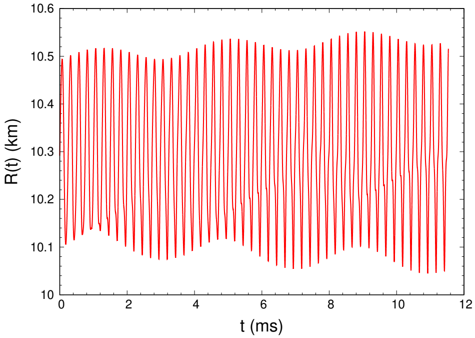

- Stellar configuration: $\rho_c^0 = 1.9891 \times 10^{18}$ kg m^{-3}, $\kappa = 4.5 \times 10^{-3}$ m^5 kg^{-1} s^{-2}
- Initial perturbation: $v(r,0) = v_0 \times r/R_0$ with $v_0 = 4116$ km s^{-1}
- Numerical parameters: $n_r = 25$, $\delta t = 5 \times 10^{-5} \times t_h$ (where $t_h \sim 0.08$ ms)

Exciting oscillation modes

1. Start from an equilibrium configuration,

2. Induce a perturbation in the fluid properties so as to excite some particular oscillation modes,

3. Follow the time evolution of a fluid variable (the central density or the radius, here).

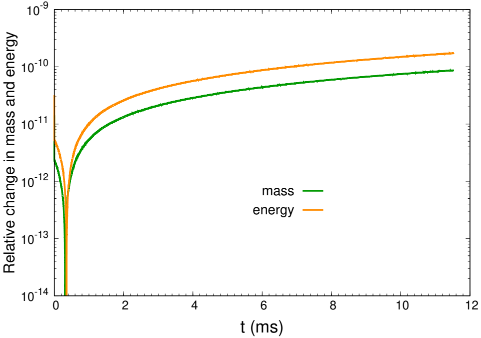

♠ Stellar configuration: $\rho_c^0 = 1.9891 \times 10^{18}$ kg m^{-3}, $\kappa = 4.5 \times 10^{-3}$ m^5 kg^{-1} s^{-2}

♠ Initial perturbation: $v(r, 0) = v_0 \times r/R_0$ with $v_0 = 4116$ km s^{-1}

♠ Numerical parameters: $n_r = 25$, $\delta t = 5 \times 10^{-5} \times t_h$ (where $t_h \sim 0.08$ ms)

Eigenmodes

Eigenmodes can be identified by Fourier transforming the time profile of some variables, *e.g.*, $R(t)$, $\rho_c(t)$, $\int \rho(r,t)dr$, ...

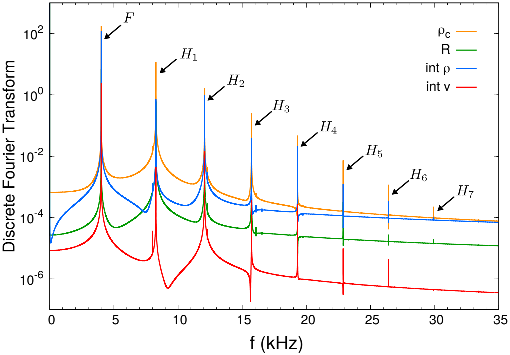

♠ Stellar configuration:

$\rho_c^0 = 1.9891 \times 10^{18}$ kg m^{-3}

$\kappa = 4.5 \times 10^{-3}$ m^5 kg^{-1} s^{-2}

♠ Initial perturbation:

$$v(r,0) = v_0 \times r/R_0$$
$$v_0 = 3 \text{ km s}^{-1}$$

♠ Numerical parameters:

$$n_r = 25,\ \delta t = 10^{-3} \times t_h$$
$$\&\ t_{\max} = 10^4 \times t_h$$

Eigenmodes

Eigenmodes can be identified by Fourier transforming the time profile of some variables, *e.g.*, $R(t)$, $\rho_c(t)$, $\int \rho(r,t)dr$, ...

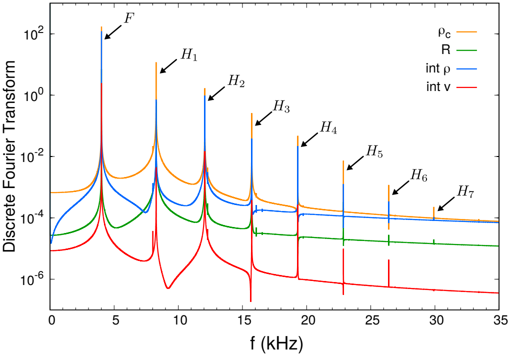

♠ Stellar configuration:

$\rho_c^0 = 1.9891 \times 10^{18}$ kg m^{-3}

$\kappa = 4.5 \times 10^{-3}$ m^5 kg^{-1} s^{-2}

♠ Initial perturbation:

$$v(r,0) = v_0 \times r/R_0$$
$$v_0 = 3 \text{ km s}^{-1}$$

♠ Numerical parameters:

$$n_r = 25,\ \delta t = 10^{-3} \times t_h$$
$$\&\ t_{\max} = 10^4 \times t_h$$

Our values for the F, H_1 and H_2 eigenfrequencies agree with those obtained by Hennig, *J. of Comp. Phys.* **235** (2013) within a few 10^{-3} %.

Non-linear harmonics

Non-linear effects occur when the initial perturbation gets stronger.

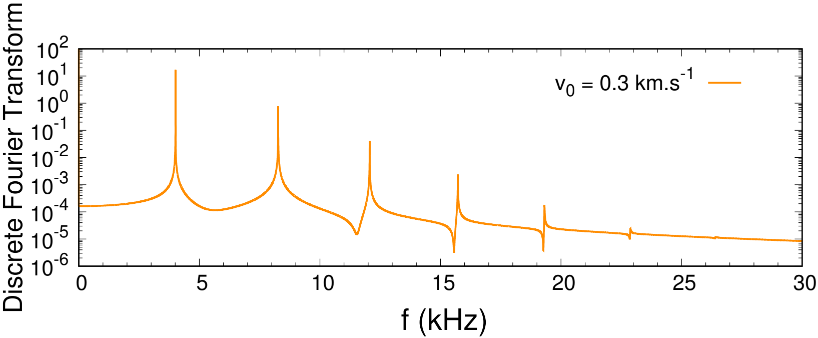

Non-linear harmonics

Non-linear effects occur when the initial perturbation gets stronger.

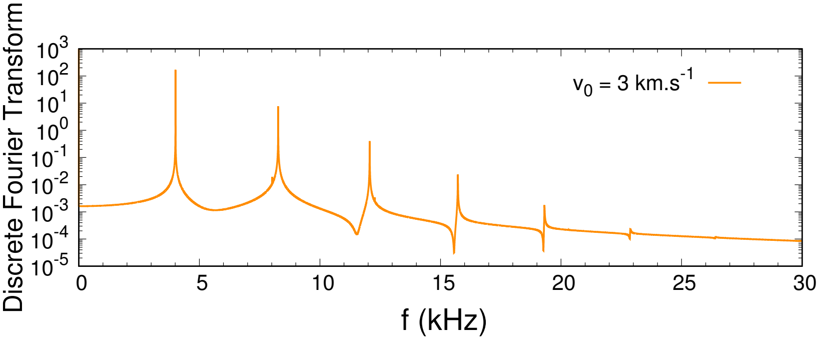

Non-linear harmonics

Non-linear effects occur when the initial perturbation gets stronger.

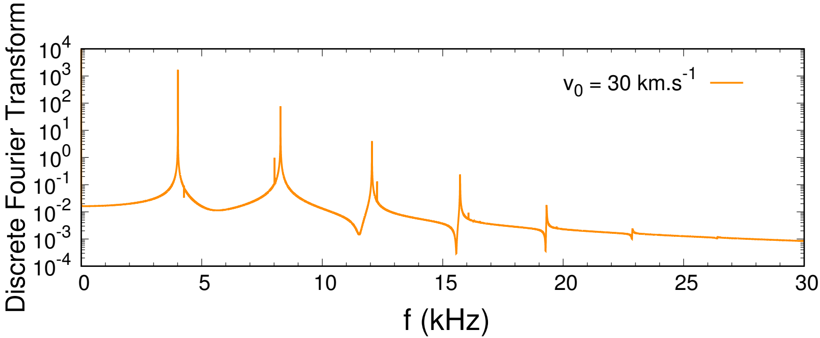

Non-linear harmonics

Non-linear effects occur when the initial perturbation gets stronger.

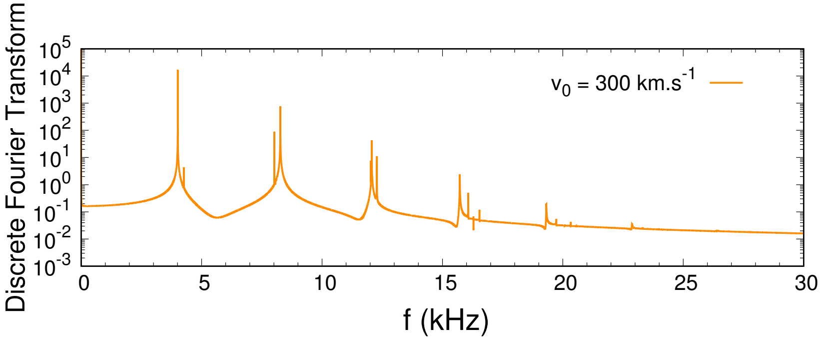

Non-linear harmonics

Non-linear effects occur when the initial perturbation gets stronger.

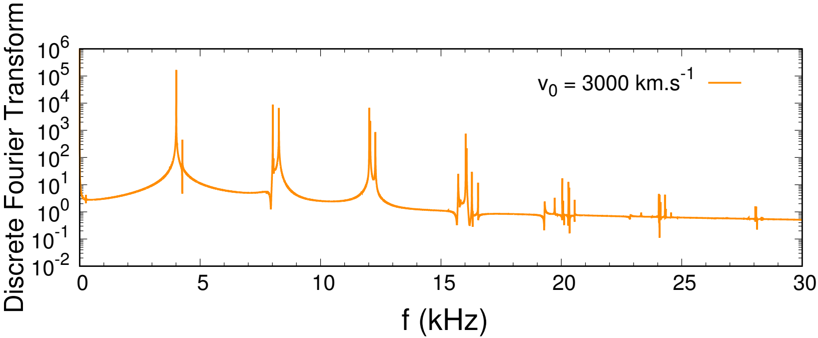

Non-linear harmonics

Non-linear effects occur when the initial perturbation gets stronger.

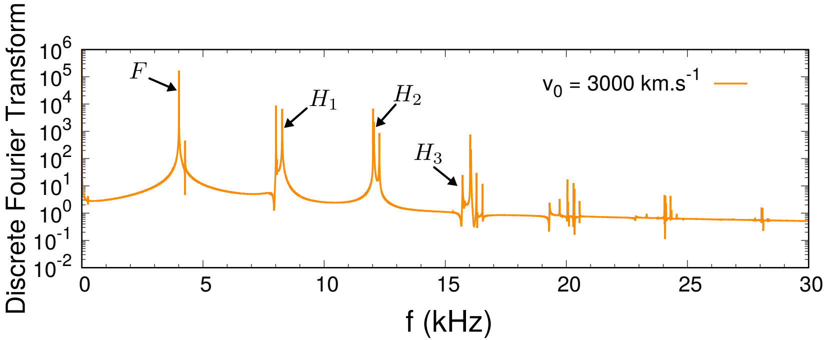

Non-linear harmonics

Non-linear effects occur when the initial perturbation gets stronger.

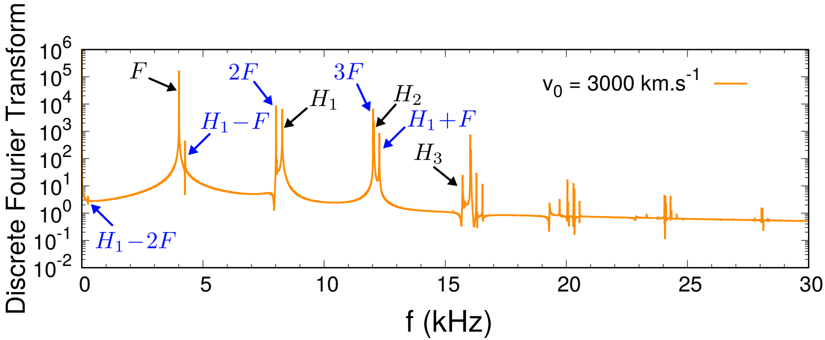

Appearance of non-linear harmonics ⇝ mode couplings.

Eigenfunction recycling

Eigenfunction recycling technique can be used to excite only one desired specific eigenmode [see Dimmelmeier *et al.*, *MNRAS* **368** (2006)].

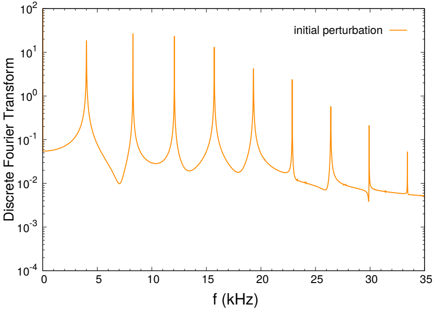

Eigenfunction recycling

Eigenfunction recycling technique can be used to excite only one desired specific eigenmode [see Dimmelmeier *et al.*, *MNRAS* **368** (2006)].

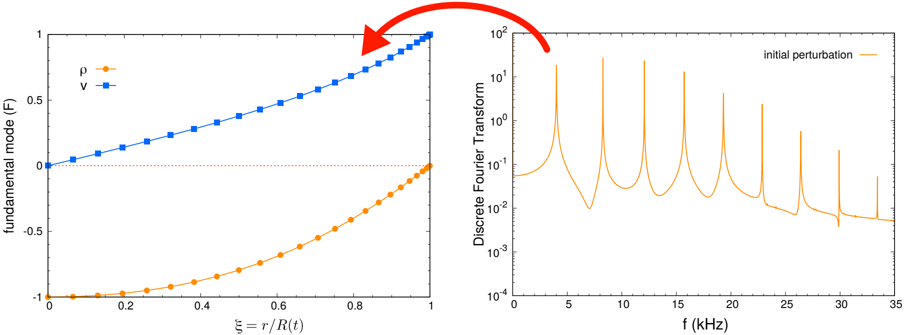

Eigenfunction recycling

Eigenfunction recycling technique can be used to excite only one desired specific eigenmode [see Dimmelmeier *et al.*, *MNRAS* **368** (2006)].

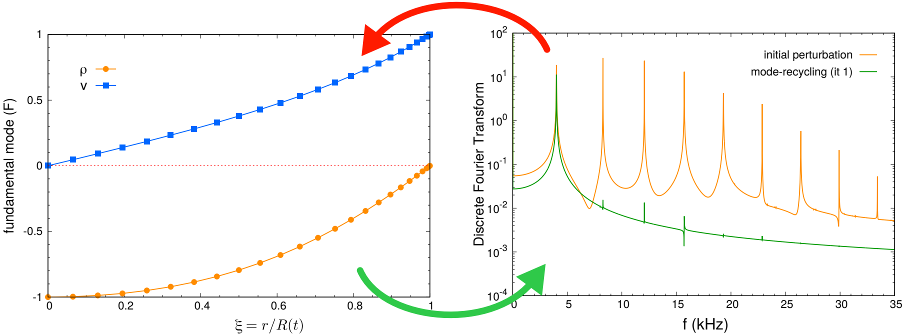

Eigenfunction recycling

Eigenfunction recycling technique can be used to excite only one desired specific eigenmode [see Dimmelmeier *et al.*, *MNRAS* **368** (2006)].

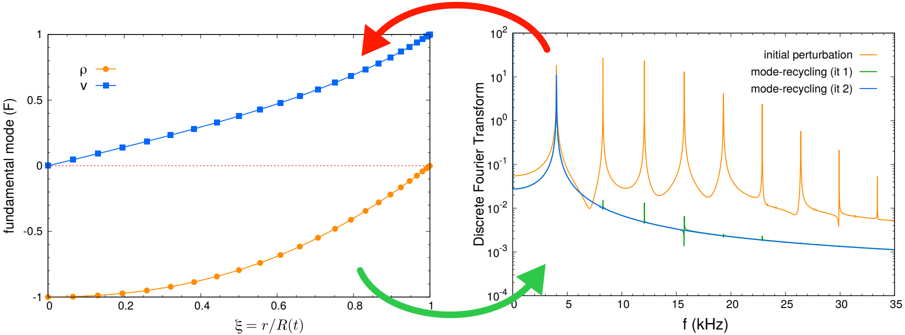

Eigenfunction recycling

Eigenfunction recycling technique can be used to excite only one desired specific eigenmode [see Dimmelmeier *et al.*, *MNRAS* **368** (2006)].

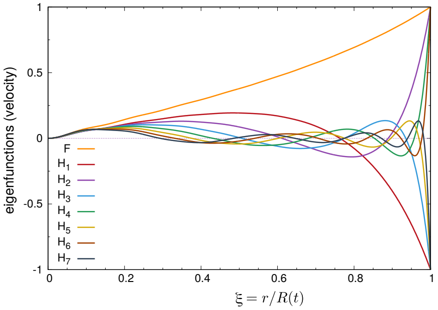

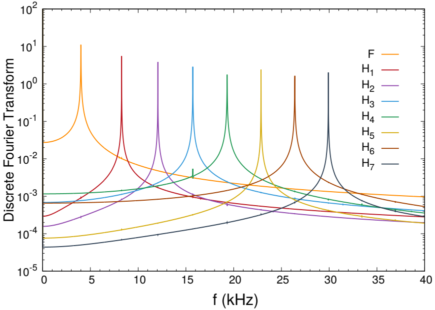

1. Neutron stars and gravitational waves
2. The first direct detection of gravitational waves from a binary neutron-star merger & tidal deformabilities
   in collaboration with N. Chamel and L. Perot (ULB)
3. Modelling neutron-star oscillations with spectral methods
   in collaboration with J. Novak, M. Oertel and E. Declerck (LUTH)
4. Conclusions

Conclusions

- Neutron stars are unique laboratories for exploring novel phases of matter under extreme conditions.

- Studying the GW emission of neutron stars can shed light on the interior of these stars.

- Some interesting constraints on the EoS have been already inferred from GW170817 (and its EM counterparts).

- The Advanced LIGO and Virgo detectors are currently in their third observation run:

  https://gracedb.ligo.org/superevents/public/O3/

Conclusions

- Neutron stars are unique laboratories for exploring novel phases of matter under extreme conditions.

- Studying the GW emission of neutron stars can shed light on the interior of these stars.

- Some interesting constraints on the EoS have been already inferred from GW170817 (and its EM counterparts).

- The Advanced LIGO and Virgo detectors are currently in their third observation run:

https://gracedb.ligo.org/superevents/public/O3/

Thank you!

Appendices

Gravitational-wave spectrum

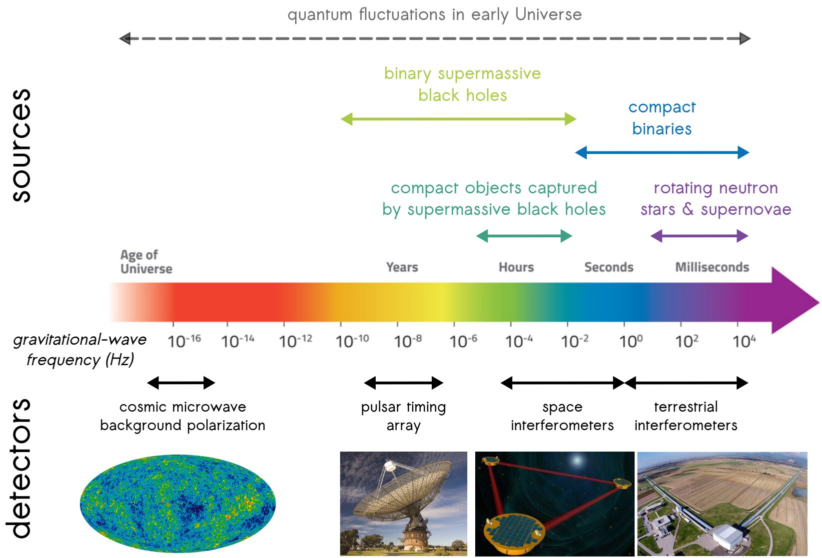

Gravitational-wave spectrum

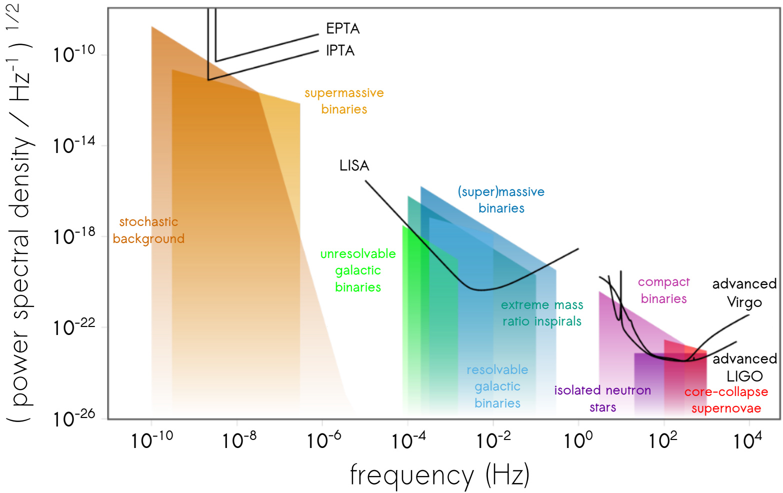

Nuclear-matter properties

Expanding the energy per nucleon of infinite nuclear matter of density $n = n_0(1+\epsilon)$ and charge asymmetry $\eta = (n_n - n_p)/n$ about the equilibrium density $n = n_0$ (= saturation density) and $\eta = 0$:

$$e(n,\eta) = a_v + \left(J + \tfrac{1}{3}L\epsilon\right)\eta^2 + \tfrac{1}{18}(K_v + \eta^2 K_{\rm sym})\epsilon^2 + \cdots$$

- Pure Neutron Matter:

$$e_{\rm NeuM}(n) \equiv e(n,1) \simeq a_v + J + \tfrac{1}{3}L\epsilon + \tfrac{1}{18}(K_v + K_{\rm sym})\epsilon^2 + \cdots$$

- Symmetric Nuclear Matter:

$$e_{\rm SNM}(n) \equiv e(n,0) = a_v + \tfrac{1}{18}K_v\epsilon^2 + \cdots$$

- Symmetry energy:

$$S(n) = e_{\rm NeuM}(n) - e_{\rm SNM}(n) \simeq J + \tfrac{1}{3}L\epsilon + \tfrac{1}{18}K_{\rm sym}\epsilon^2 + \cdots$$

Nuclear-matter properties for the BSk EoSs

	BSk19	BSk20	BSk21	BSk22	BSk23	BSk24	BSk25	BSk26
J [MeV]	30.0	30.0	30.0	32.0	31.0	30.0	29.0	30.0
L [MeV]	31.9	37.4	46.6	68.5	57.8	46.4	36.9	37.5
K_v [MeV]	237.3	241.4	245.8	245.9	245.7	245.5	236.0	240.8
$K_{\rm sym}$ [MeV]	-191.4	-136.5	-37.2	13.0	-11.3	-37.6	-28.5	-135.6
NeuM	FP	APR	LS2	LS2	LS2	LS2	LS2	APR

- J = symmetry-energy coefficient (at saturation),
- L = slope of the symmetry energy,
- K_v = incompressibility coefficient,
- $K_{\rm sym}$ = symmetry incompressibility coefficient.

★ FP = Friedman & Pandharipande, *Nucl. Phys. A* **361** (1981),

★ APR = 'A18 + δv + UIX*' EoS of Akmal *et al.*, *PRC* **58** (1998),

★ LS2 = 'V18' EoS of Li & Schulze, *PRC* **78** (2008).

More details can be found in Potekhin *et al.*, *A&A* **560** (2013) and Pearson *et al.*, *MNRAS* **481** (2018).

Pure Neutron Matter

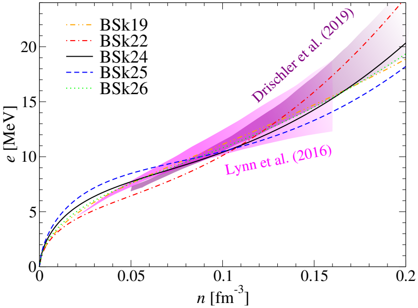

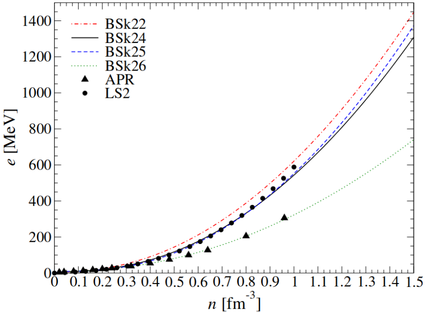

Symmetry energy

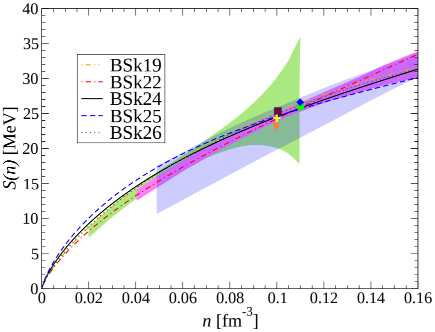

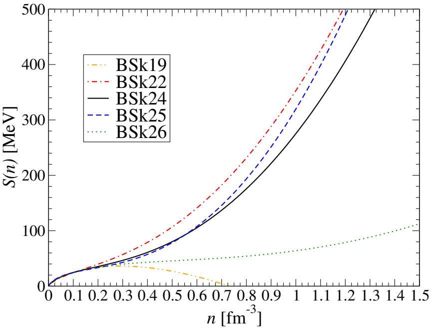

Tidal deformations

During the last orbits preceding the merger, the two neutron stars are strongly deformed by tidal effects.

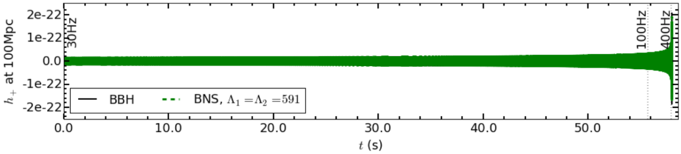

Tidal deformations

During the last orbits preceding the merger, the two neutron stars are strongly deformed by tidal effects.

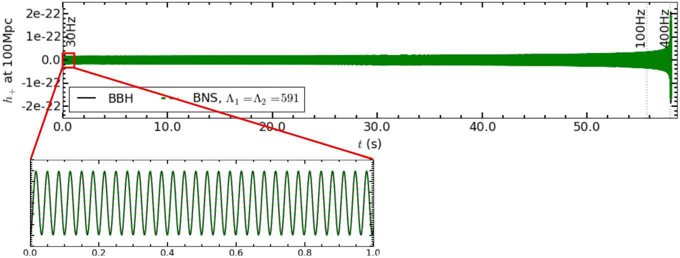

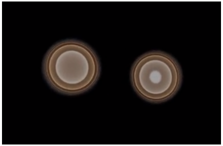

Tidal deformations

During the last orbits preceding the merger, the two neutron stars are strongly deformed by tidal effects.

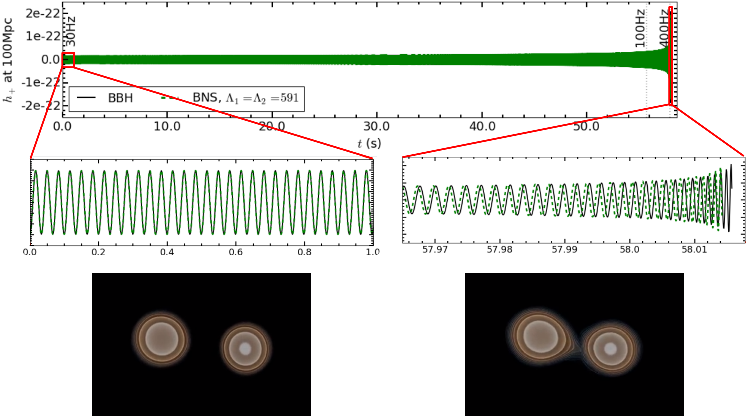

Computing tidal deformabilities (1/2)

- TOV equations:

$$\frac{\mathrm{d}P(r)}{\mathrm{d}r} = -\frac{G\,\mathcal{E}(r)m(r)}{c^2r^2}\left[1+\frac{P(r)}{\mathcal{E}(r)}\right]\left[1+\frac{4\pi P(r)r^3}{c^2m(r)}\right]\left[1-\frac{2Gm(r)}{c^2r}\right]^{-1},$$

$$m(r) = \frac{4\pi}{c^2}\int_0^r \mathcal{E}(r')r'^2\,\mathrm{d}r'\,,$$

- Additional equation for Λ:

$$H''(r) + H'(r)f(r) + H(r)g(r) = 0\,,$$

- Boundary conditions:

$$m\,(0) = 0\,,\;\; \mathcal{E}\,(0) = \mathcal{E}_c\,,\;\; H(0) = 0 \text{ and } H'(0) = 0\,.$$

Computing tidal deformabilities (2/2)

- Love number:

$$k_2 = \frac{8C^5}{5}(1-2C)^2\left[2+2C(y-1)-y\right]\Big\{2C\left[6-3y+3C(5y-8)\right] + 4C^3\left[13-11y+C(3y-2)+2C^2(1+y)\right] + 3(1-2C)^2\left[2-y+2C(y-1)\right]\ln(1-2C)\Big\}^{-1},$$

where $y \equiv R\,H'(R)/H(R)$ and C is the compactness parameter of the star.

- The Love number and the tidal deformability are related through:

$$\Lambda = \frac{2}{3}k_2\left(\frac{c^2R}{GM}\right)^5 .$$

Love numbers

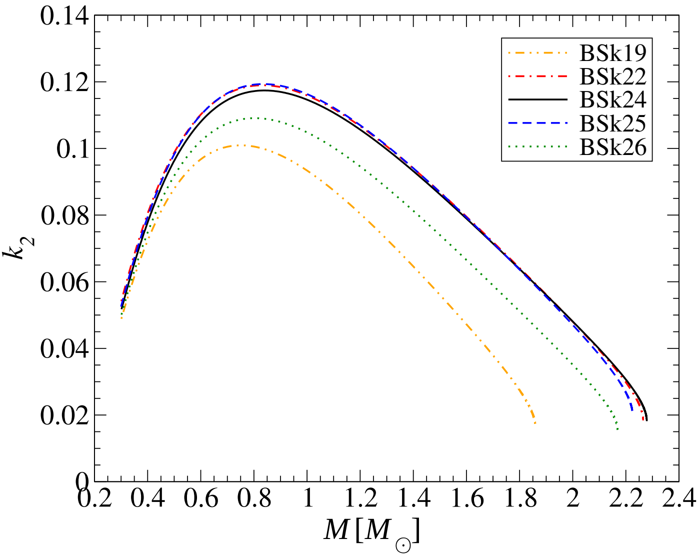

Tidal deformability of a $1.4M_\odot$ NS

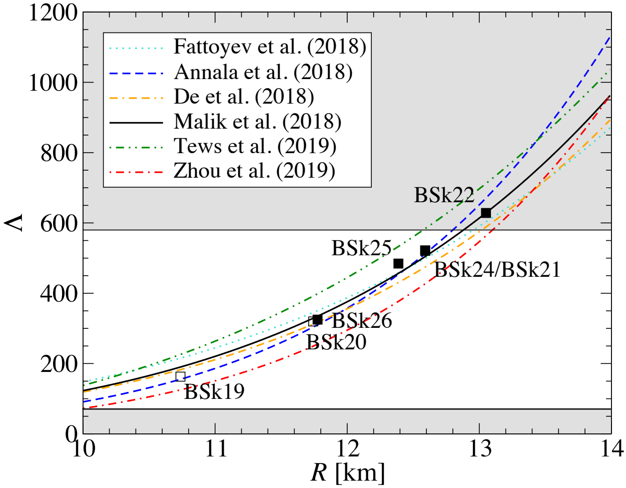

Constraints on $M_{\rm max}$

★ Different analyses of the short gamma-ray burst and of the kilonova emission, combined with the total binary mass $M_{\rm tot} = 2.74^{+0.04}_{-0.01}\ M_\odot$ inferred from the GW signal, have led to constraints on the maximum mass of a nonrotating NS.

★ Assuming the formation of a short-lived NS, Margalit & Metzger (2017) obtained $M_{\rm max} \lesssim 2.17\ M_\odot$, Rezzolla *et al.* (2018) $M_{\rm max} \lesssim 2.16^{+0.17}_{-0.15}\ M_\odot$, and Ruiz *et al.* (2018) $2.16 \pm 0.23\ M_\odot \lesssim M_{\rm max} \lesssim 2.28 \pm 0.23\ M_\odot$.

★ Shibata *et al.* (2017, 2019) obtained compatible estimates, namely $2.1\ M_\odot \lesssim M_{\rm max} \lesssim 2.3\ M_\odot$, under the assumption of a longer-lived NS (with a lifetime up to tens of seconds).

★ Alternatively, other authors have interpreted the late-time electromagnetic emission in terms of a very long-lived NS remnant (with a lifetime of about 20 days) and concluded that $M_{\rm max} \gtrsim 2.6\ M_\odot$ (see, e.g., Yu *et al.* (2018)).

Any firm conclusion on the EoS can hardly be drawn in view of the lack of consensus on the interpretation of the EM counterparts of GW170817.

Constraints on R

★ The amount of material ejected during the collision, i.e. $\sim 0.02 - 0.05\ M_\odot$, inferred from observations of the EM counterpart of GW170817 points against a prompt collapse to a black hole. The total mass $M_{\rm tot} = M_1 + M_2$ should thus be lower than some threshold value $M_{\rm thres}$.

★ Combining $M_{\rm tot} = 2.74^{+0.04}_{-0.01}\ M_\odot$ with an empirical relation for $M_{\rm thres}$, Bauswein *et al.* (2017) obtained the lower limit: $R_{1.6} \geq 10.30^{+0.15}_{-0.03}$ km.

Assuming further that the remnant lived for more than 10 ms, they obtained the more stringent constraint $R_{1.6} \geq 10.68^{+0.15}_{-0.04}$ km.

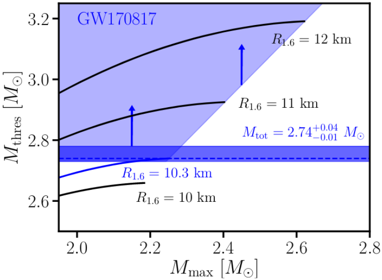

★ Using a different empirical relation for $M_{\rm thres}$ but similar arguments, Köppel *et al.* (2019) derived a tighter bound on NS radii: $R \geq -0.88M^2 + 2.66M + 8.91$ km for $1.2\ M_\odot < M < 2\ M_\odot$.

Tests of convergence

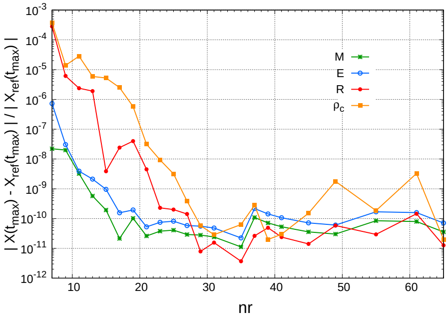

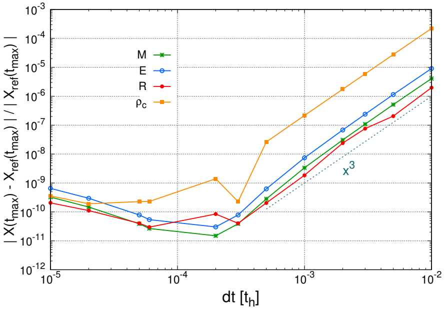

Spectral convergence ('exact' results correspond to 33 collocation points)

Third-order scheme ('exact' results correspond to $\delta t = 10^{-4} \times t_h$)

Eigenfunctions

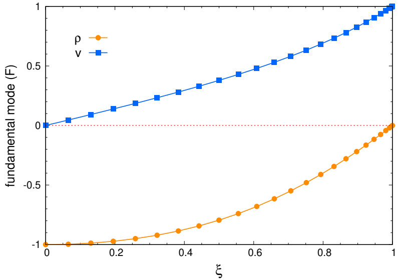

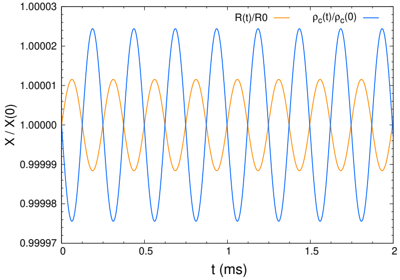

The eigenfunction of v corresponding to the H_i-mode has i nodes.

Eigenfunctions

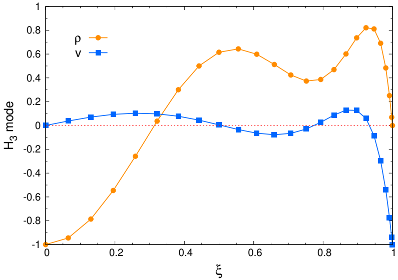

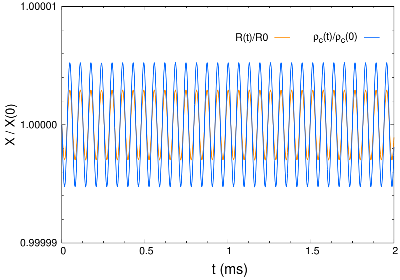

The eigenfunction of v corresponding to the H_i-mode has i nodes.

Eigenfunctions

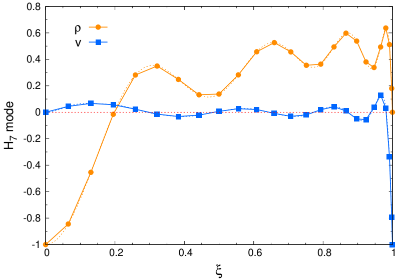

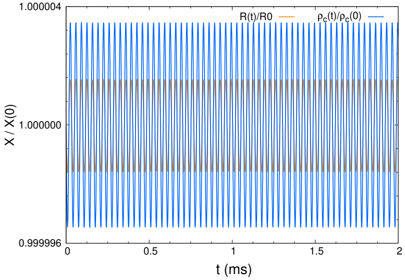

The eigenfunction of v corresponding to the H_i-mode has i nodes.

Cowling approximation

Cowling approximation: $\Phi(r,t) = \Phi(r,0), \ \forall t.$

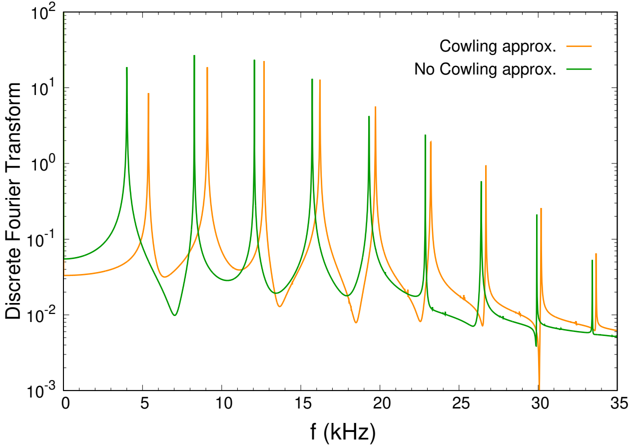

Cowling approximation

Cowling approximation: $\Phi(r,t) = \Phi(r,0), \ \forall t.$